

The Use of Fly Ash for the Control and Treatment of Acid Mine Drainage

Kelley Reynolds

Senior Microbiologist, Eskom Enterprises – TSI Division, Private Bag 40175, Cleveland, 2022

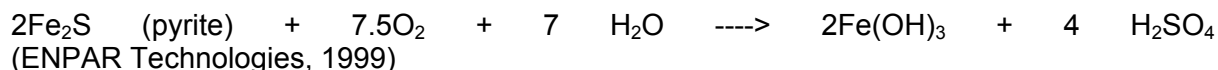
Summary

This report details the results of laboratory scale column tests to determine the feasibility of utilising fly ash to treat and control acid mine drainage (AMD) flow. AMD emanates from many open cast coal mines, when pyritic rock is exposed to the atmosphere. The oxidation of these rocks and the subsequent contact with water, either from rain or underground sources, forms an effluent with a pH often below 2 and high sulphate concentrations. As this effluent flows through the surrounding strata, heavy metals, present in the rocks, are leached out. Approximate 700 000m³ of AMD flows into the Loskop Dam annually alone.

Eskom produces approximately 22 million tons of fly ash annually. For the most part this ash is dumped on ash dumps/dams which have to be rehabilitated. The highly alkaline nature of fly ash is well known as is its buffering nature. It is envisaged that the ash be used as a walling material, initially to treat the AMD and secondly to act as a dam to redirect the AMD flow.

1. INTRODUCTION

Acid Mine/Rock Drainage (AMD or ARD) is one of the biggest environmental problems facing the mining industry today. AMD is produced as a result of the oxidation of sulphide rich mine tailings and the subsequent contact with water to produce sulphuric acid. The most common sulphate is Fe₂SO₄ (Pyrite). This reaction is usually catalysed by bacteria and proceeds according to the following general equation (ENPAR Technologies, 1999).



The exact process equations are very complex (White, 2000) and several minor variations are available (Evangelou and Zhang, 1995). The one consistent point in the literature is the role of bacteria in the oxidative process (White, 2000). Nordstrom and Southam (1997) have listed 22 species, which are known to be associated with mine waters. The most common of these is *Thiobacillus ferrooxidans* (O'Brien, 2000). This bacteria metabolises inorganic compounds, including sulphides (White, 2000). *T. ferrooxidans* is classified as an acidophilic lithotroph, an acid tolerant microorganism that gains energy from the oxidation of inorganic compounds (Nordstrom and Southam, 1997). It is thus through their natural behavior that these microorganisms catalyse the AMD producing reactions (White, 2000).

The metal load of the leachate varies dependent of the surrounding strata. In some cases the rock may have a buffering effect and the resultant effluent is neutral (O'Brien, 2000). Generally, however, the leachate has a very low pH of approximately 2 or lower and a total dissolved solids of 4000-5000mg/L. In addition, the sulphate concentrations are normally in the thousands of mg/L (Gericke *et al*, 2001).

It is estimated that approximately 54% of rainfall in the Witbank catchment percolates through the mine spoils. This relates to 700 000m³ of highly polluted water flowing into the Loskop Dam (Bullock and Bell, 1997).

Various methods have been considered to treat this water, ranging from lime neutralisation (Gericke *et al*, 2001) to electrochemical protection (Pulles *et al*, 1996). These forms of treatment are costly and require constant management (Anon, 2000). The water produced after these treatments can only be utilised for irrigation and this only if the heavy metals have been removed sufficiently (Gericke *et al*, 2001).

The 100 million tons of low grade coal burnt in Eskom power stations annually produces approximately 22 million tons of inorganic fly ash (Willis, 1999). This waste creates huge disposal problems and at present is heaped on ash dumps except for a small percentage that is used in the building industry (Reynolds, 1999).

Eskom power stations are generally built near to the colliery supplying the coal and the two waste streams are in close proximity. Fly ash has been used historically as a supplement to backfill to reduce AMD (Proposed ASTM guide, 1999).

2. MATERIALS AND METHODS

Acid Mine Drainage samples were obtained from a Mpumalanga Mine. The mine has a complex water catchment system which allows for regular samples to be collected. At the moment the AMD is treated in a liming process and the resultant sludge is stored. This means of treatment is however expensive and the resulting sludge contains heavy metals.

Fly ash was obtained from various power stations. The selection of the relevant power station was on the basis of fly ash particle size. Initially coarser ash was used followed by the finest. Due to the coarse nature of the ash it is believed that the AMD will percolate though relatively easily, in this way treating the water. As the AMD flow continues the fly ash will be clogged as a result of precipitation and the pozzalanic effect of the ash. This clogging will be more evident in the finer ash tests.

The fly ash was packed into duplicate columns of four lengths and settled by means of an orbital shaker. The weight of the column before and after filling was noted to ensure that the duplicate test contained the same amount of ash.

The AMD was gravity feed through all eight columns simultaneously. In this way a constant head was maintained.

As the water passed out of the ash column, it was collected and analysed for pH, conductivity, sulphates and heavy metals. The analyses were conducted daily initially and weekly to two weekly thereafter. The analyses were continued until the pH of the exiting AMD dropped below 8.5 for the coarse ash and until the columns blocked for the fine ash.

Once the pH had dropped sufficiently the flow through the columns was stopped and the ash removed. The ash was then sampled from the top, middle and bottom of the extracted column.

3. RESULTS AND CONCLUSIONS

Table 1 shows the parameters of a typical AMD and Fly ash.

Table 1. Parameters of the initial AMD and Fly ash

Parameter	Value
AMD	
pH	2.88
Sulphate (mg/L)	3654
Conductivity (mS/cm)	4.7
Al (mg/L)	33.5
B (mg/L)	0.06
Ba (mg/L)	0.01
Be (mg/L)	<0.005
Cd (mg/L)	0.04
Co (mg/L)	0.54
Cr (mg/L)	<0.005
Cu (mg/L)	0.05
Fe (mg/L)	122
Mn (mg/L)	43
Ni (mg/L)	0.68
Pb (mg/L)	0.03
Sr (mg/L)	0.71
Zn (mg/L)	2.8
Fly ash	
pH	11.34
Conductivity (mS/cm)	0.676

Once the AMD was passed into the columns they had to be sealed to withstand the water pressure of the head of water, as the AMD did not pass directly through the ash.

From the onset of the AMD addition iron deposition was noted on the surface of the ash

The results obtained from the treated AMD (leachate), indicated that the pH of the AMD passing the ash column was raised to greater than 12. This indicates the buffering ability of the fly ash.

Once above pH 12, the pH of the leachate from the shortest columns immediately began to drop. The duplicate tests followed the same trends in both experiments but were not the same. The reason for the difference in the pHs is not clear, initially it was considered that channeling had occurred but as there was no increase in the heavy metal concentrations, this was disregarded. The columns show reducing pHs in correlation to the column length, that is, the longer the column, the higher the pH remains.

The conductivity (EC), in the coarse ash experiments remained relatively constant after an initial high peak experienced in all columns. For the fine ash experiments however the EC increased slightly and then decreased steadily until the columns clogged.

All of the leachates of the coarse ash experiment show an initial decrease in the sulphate concentrations. This is due to the formation of CaSO_4 on reaction with the fly ash. The sulphate concentrations in the shorter columns started to increase after the initial reduction. This is believed to be due to the pH of the leachate becoming too low which solubilises the CaSO_4 . The longer columns maintained the low sulphate levels for a longer period and at the time of this report had not shown any increased sulphate.

In the fine ash experiments however, the columns blocked after 46 days and no increase in sulphate concentrations had been noted by that time.

In general the heavy metal concentrations decreased. Beryllium, Cadmium, Cobalt, Lead and Nickel concentrations were all low and decreased to undetectable levels.

The concentration of aluminium decreased from 33.5 mgL⁻¹ to 1mgL⁻¹ in the coarse ash experiments and from 275mg.L⁻¹ to below 10mg.L⁻¹ in the fine ash experiments. It is believed that the aluminium reacts with the silica in the ash and forms Mullite.

Barium concentrations showed a slight increase but remained in a very low concentration for the coarse ash but are highly erratic in the fine ash work.

The Boron concentrations increased with coarse ash and decreased slightly with fine ash. It is believed that the Boron is detected due to its high motility at such high pH's.

The Chromium concentrations show an initial increase in concentration, followed by a reduction, in both experiments. The peak concentration is reached after a longer duration in the longer columns in the coarse work. This may be due to the fact that the columns take longer to break through and the Chromium would be carried in the initial AMD to pass the molecule. It is also noted that the longer the column the higher the peak concentration. This can be attributed to the fact that the AMD would have been in contact with more fly ash and thus been able to collect any possible Chromium from the ash.

The fine ash experiments indicated a similar initial spike but the Chromium levels were below 0.1mgL⁻¹ after day 15.

The Copper concentrations in the coarse work indicated an initial increase as any soluble copper is passed through the column, followed by an equally quick reduction to lower stabilised levels, when the concentration is more fixed.

The fine work shows a reduction in concentrations followed by a slow increase before the columns clogged.

Iron concentrations decrease significantly from 122 mgL⁻¹ to 0.01 mgL⁻¹ for the coarse work and from 4000mgL⁻¹ to below 3mgL⁻¹ in the fine work. This may be due to the formation of Hematite on the top of the columns.

The Manganese results show an immediate decrease in the concentrations from 43 mgL⁻¹ to near the detection limit of 0.005mgL⁻¹ and from 35mgL⁻¹ to below 0.1mgL⁻¹ for the coarse and fine ash experiments respectively.

The concentrations for Zinc also decreased after passing through the column. The concentrations dropped from 2.8 mgL⁻¹ to 0.1 mgL⁻¹ through coarse ash and from 6.3mgL⁻¹ to below 2mgL⁻¹ through fine.

Once the pH of the columns fell below 8.5 the flow was stopped and samples taken from the top, middle and bottom of the column. The various samples of the extracted ash column were submitted for XRF, XRD and Electron Microscopic analysis to determine the change in mineralogy.

The results of the XRF and XRD analyses on the ash samples are shown in Tables 2 and 3. The XRD analyses showed that gypsum (CaSO₄) is being formed at the top of the columns. This may be due to the presence of the sulphuric acid at the top of the column. The H₂SO₄ reacts with the Ca and forms Gypsum.

Table 2: XRD analysis of the shortest columns. With coarse ash

Sample	Major Phase	Minor Phase
Fly ash	Mullite $\text{Al}_6\text{Si}_2\text{O}_{13}$ Quartz SiO_2	Not detected
A0.5 Top	Gypsum $\text{CaSO}_4 \cdot 2\text{H}_2\text{O}$ Hematite Fe_2O_3	Mullite $\text{Al}_6\text{Si}_2\text{O}_{13}$ Quartz SiO_2
B0.5 Top	Gypsum $\text{CaSO}_4 \cdot 2\text{H}_2\text{O}$ Hematite Fe_2O_3	Mullite $\text{Al}_6\text{Si}_2\text{O}_{13}$ Quartz SiO_2
A0.5 Middle	Gypsum $\text{CaSO}_4 \cdot 2\text{H}_2\text{O}$ Hematite Fe_2O_3	Mullite $\text{Al}_6\text{Si}_2\text{O}_{13}$ Quartz SiO_2
B0.5 Middle	Gypsum $\text{CaSO}_4 \cdot 2\text{H}_2\text{O}$ Hematite Fe_2O_3	Mullite $\text{Al}_6\text{Si}_2\text{O}_{13}$ Quartz SiO_2
A0.5 Bottom	Gypsum $\text{CaSO}_4 \cdot 2\text{H}_2\text{O}$ Hematite Fe_2O_3	Mullite $\text{Al}_6\text{Si}_2\text{O}_{13}$ Quartz SiO_2
B0.5 Bottom	Gypsum $\text{CaSO}_4 \cdot 2\text{H}_2\text{O}$ Hematite Fe_2O_3	Mullite $\text{Al}_6\text{Si}_2\text{O}_{13}$ Quartz SiO_2
A1.0 Top	Gypsum $\text{CaSO}_4 \cdot 2\text{H}_2\text{O}$ Hematite Fe_2O_3	Mullite $\text{Al}_6\text{Si}_2\text{O}_{13}$ Quartz SiO_2
B1.0 Top	Gypsum $\text{CaSO}_4 \cdot 2\text{H}_2\text{O}$ Hematite Fe_2O_3	Mullite $\text{Al}_6\text{Si}_2\text{O}_{13}$ Quartz SiO_2
A1.0 Middle	Gypsum $\text{CaSO}_4 \cdot 2\text{H}_2\text{O}$ Hematite Fe_2O_3	Mullite $\text{Al}_6\text{Si}_2\text{O}_{13}$ Quartz SiO_2
B1.0 Middle	Gypsum $\text{CaSO}_4 \cdot 2\text{H}_2\text{O}$ Hematite Fe_2O_3	Mullite $\text{Al}_6\text{Si}_2\text{O}_{13}$ Quartz SiO_2
A1.0 Bottom	Gypsum $\text{CaSO}_4 \cdot 2\text{H}_2\text{O}$ Hematite Fe_2O_3	Mullite $\text{Al}_6\text{Si}_2\text{O}_{13}$ Quartz SiO_2
B1.0 Bottom	Gypsum $\text{CaSO}_4 \cdot 2\text{H}_2\text{O}$ Hematite Fe_2O_3	Mullite $\text{Al}_6\text{Si}_2\text{O}_{13}$ Quartz SiO_2
A1.5 Top	Gypsum $\text{CaSO}_4 \cdot 2\text{H}_2\text{O}$ Hematite Fe_2O_3	Mullite $\text{Al}_6\text{Si}_2\text{O}_{13}$ Quartz SiO_2
B1.5 Top	Gypsum $\text{CaSO}_4 \cdot 2\text{H}_2\text{O}$ Hematite Fe_2O_3	Mullite $\text{Al}_6\text{Si}_2\text{O}_{13}$ Quartz SiO_2
A1.5 Middle	Gypsum $\text{CaSO}_4 \cdot 2\text{H}_2\text{O}$ Hematite Fe_2O_3	Mullite $\text{Al}_6\text{Si}_2\text{O}_{13}$ Quartz SiO_2
B1.5 Middle	Gypsum $\text{CaSO}_4 \cdot 2\text{H}_2\text{O}$ Hematite Fe_2O_3	Mullite $\text{Al}_6\text{Si}_2\text{O}_{13}$ Quartz SiO_2
A1.5 Bottom	Gypsum $\text{CaSO}_4 \cdot 2\text{H}_2\text{O}$ Hematite Fe_2O_3	Mullite $\text{Al}_6\text{Si}_2\text{O}_{13}$ Quartz SiO_2
B1.5 Bottom	Gypsum $\text{CaSO}_4 \cdot 2\text{H}_2\text{O}$ Hematite Fe_2O_3	Mullite $\text{Al}_6\text{Si}_2\text{O}_{13}$ Quartz SiO_2

The XRF analysis showed very slight differences of the columns to the original fly ash. The only marked variation is that of Ca which was high in the fly ash but lower in the column. In addition the Ca concentration increased down the column. This may be due to the formation of gypsum at the top of the column.

Table 3: XRF analysis of the coarse work columns.

Sample	Major Phase	Minor Phase
Fly ash	Mullite $\text{Al}_6\text{Si}_2\text{O}_{13}$ Quartz SiO_2	Not detected
A0.5 Top	Gypsum $\text{CaSO}_4 \cdot 2\text{H}_2\text{O}$ Hematite Fe_2O_3	Mullite $\text{Al}_6\text{Si}_2\text{O}_{13}$ Quartz SiO_2
B0.5 Top	Gypsum $\text{CaSO}_4 \cdot 2\text{H}_2\text{O}$ Hematite Fe_2O_3	Mullite $\text{Al}_6\text{Si}_2\text{O}_{13}$ Quartz SiO_2
A0.5 Middle	Gypsum $\text{CaSO}_4 \cdot 2\text{H}_2\text{O}$ Hematite Fe_2O_3	Mullite $\text{Al}_6\text{Si}_2\text{O}_{13}$ Quartz SiO_2
B0.5 Middle	Gypsum $\text{CaSO}_4 \cdot 2\text{H}_2\text{O}$ Hematite Fe_2O_3	Mullite $\text{Al}_6\text{Si}_2\text{O}_{13}$ Quartz SiO_2
A0.5 Bottom	Gypsum $\text{CaSO}_4 \cdot 2\text{H}_2\text{O}$ Hematite Fe_2O_3	Mullite $\text{Al}_6\text{Si}_2\text{O}_{13}$ Quartz SiO_2
B0.5 Bottom	Gypsum $\text{CaSO}_4 \cdot 2\text{H}_2\text{O}$ Hematite Fe_2O_3	Mullite $\text{Al}_6\text{Si}_2\text{O}_{13}$ Quartz SiO_2
A1.0 Top	Gypsum $\text{CaSO}_4 \cdot 2\text{H}_2\text{O}$ Hematite Fe_2O_3	Mullite $\text{Al}_6\text{Si}_2\text{O}_{13}$ Quartz SiO_2
B1.0 Top	Gypsum $\text{CaSO}_4 \cdot 2\text{H}_2\text{O}$ Hematite Fe_2O_3	Mullite $\text{Al}_6\text{Si}_2\text{O}_{13}$ Quartz SiO_2
A1.0 Middle	Gypsum $\text{CaSO}_4 \cdot 2\text{H}_2\text{O}$ Hematite Fe_2O_3	Mullite $\text{Al}_6\text{Si}_2\text{O}_{13}$ Quartz SiO_2
B1.0 Middle	Gypsum $\text{CaSO}_4 \cdot 2\text{H}_2\text{O}$ Hematite Fe_2O_3	Mullite $\text{Al}_6\text{Si}_2\text{O}_{13}$ Quartz SiO_2
A1.0 Bottom	Gypsum $\text{CaSO}_4 \cdot 2\text{H}_2\text{O}$ Hematite Fe_2O_3	Mullite $\text{Al}_6\text{Si}_2\text{O}_{13}$ Quartz SiO_2
B1.0 Bottom	Gypsum $\text{CaSO}_4 \cdot 2\text{H}_2\text{O}$ Hematite Fe_2O_3	Mullite $\text{Al}_6\text{Si}_2\text{O}_{13}$ Quartz SiO_2
A1.5 Top	Gypsum $\text{CaSO}_4 \cdot 2\text{H}_2\text{O}$ Hematite Fe_2O_3	Mullite $\text{Al}_6\text{Si}_2\text{O}_{13}$ Quartz SiO_2
B1.5 Top	Gypsum $\text{CaSO}_4 \cdot 2\text{H}_2\text{O}$ Hematite Fe_2O_3	Mullite $\text{Al}_6\text{Si}_2\text{O}_{13}$ Quartz SiO_2
A1.5 Middle	Gypsum $\text{CaSO}_4 \cdot 2\text{H}_2\text{O}$ Hematite Fe_2O_3	Mullite $\text{Al}_6\text{Si}_2\text{O}_{13}$ Quartz SiO_2
B1.5 Middle	Gypsum $\text{CaSO}_4 \cdot 2\text{H}_2\text{O}$ Hematite Fe_2O_3	Mullite $\text{Al}_6\text{Si}_2\text{O}_{13}$ Quartz SiO_2
A1.5 Bottom	Gypsum $\text{CaSO}_4 \cdot 2\text{H}_2\text{O}$ Hematite Fe_2O_3	Mullite $\text{Al}_6\text{Si}_2\text{O}_{13}$ Quartz SiO_2
B1.5 Bottom	Gypsum $\text{CaSO}_4 \cdot 2\text{H}_2\text{O}$ Hematite Fe_2O_3	Mullite $\text{Al}_6\text{Si}_2\text{O}_{13}$ Quartz SiO_2

The SEM analysis showed the inclusion of particles onto the, normally totally smooth, ash beads in the bottom and middle samples, the top samples showed less inclusion. It is believed that the attached particles are washed down the column by the AMD. The pHs, at the different points, in the column allow them to reattach lower down the column.

At the time of completing the report the fine work XRF and XRD results were not available.

CONCLUSIONS

The use of fly ash to treat AMD has been proven effective with fly ash on Mpumalanga AMD. The sulphates and heavy metals are reduced and the pH increased.

REFERENCES

ANON, Proposed ASTM standard guide for the use of coal combustion products for surface mine reclamation, American Coal Ash Association, 1999.

Bullock SET and Bell FG, Environmental Geology, 33

ENPAR Technologies, Electrochemical Cover to Remediate Acid Mine Drainage, ENPAR Technologies Inc, 449 Laird Road, Unit 12, Guelph, Ontario, Canada, N1G4W1. 1999.

Evangelou and Zhang

GAI Consultants, Inc, Fly Ash structural fill handbook, Electric Power Research Institute, EPRI EZ-1281, Palo Alto, CA, Dec 1979.

Gericke G, Petrik L and White R, Simultaneous Neutralisation of two harmful effluents, fly ash and acid mine drainage, for water beneficiation: A site specific case at Arnot Power Station, Eskom Resources and Strategy, Project Proposal.2002

Nordstrom DK and Southam G, Geomicrobiology of sulphide mineral oxidation. In: BANFIELD, JF and NEALSON KH (Eds) Geomicrobiology: Interactions Between Microbes and Minerals. Mineralogical Society of America, Washington DC, 361-390, 1997.

O'Brien RD, The Neutralisation of Acid Mine Drainage by Fly Ash. Unpublished MSc Thesis, University of Cape Town, RSA, 2000.

Pulles W, Howie D, Otto D and Easton J, A manual on mine water treatment and management practices in South Africa. Appendix Volume 1: Literature Reviews. WRC Report No 527/1/96.

Reynolds KA, SLASH Field Trials, Research Report RES/RR/99/00054, Eskom Technology Services International, 1999.

Dr Richard Kruger, New Products Development Manager, Ash Resources, PO Box 3017, Randburg, 2194.

White RA, Behaviour of the rare earth elements in ochreous mine drainage: a laboratory and field study. Unpublished PhD, University of Wales, Aberystwyth, UK, 2000.

Willis J, Lectures given as part of the Environmental Geochemistry Masters course, Geological Sciences, University of Cape Town, 1999.